Room-temperature Fano resonance tunable by chemical doping in few-layer graphene synthesized by chemical-vapor deposition

Zhihong Liu,[1] Xiaoxiang Lu,[1] Peng Peng,[1] Wei Wu,[1,2] Shin-Shem Pei,[1,2] Qingkai Yu,[1,2,*] and Jiming Bao[1,†]
[1]*Department of Electrical and Computer Engineering, University of Houston, Houston, Texas 77204, USA*
[2]*Center for Advanced Materials, University of Houston, Houston, Texas 77204, USA*
(Received 5 August 2010; revised manuscript received 13 September 2010; published 18 October 2010)

We report the observation of Fano-type phonon resonance using infrared Fourier transform spectroscopy at room temperature in few-layer (~3) graphene synthesized by chemical-vapor deposition on copper substrate. We subsequently demonstrate a continuous tuning of Fano line shape from antiresonance to phonon dominated by ammonia chemical doping. The few-layer Fano resonance exhibits a strong asymmetric characteristic between *n*-doped and *p*-doped graphene, different from that observed in double-layer graphene gated by external electrodes. This asymmetry probably arises from nonuniform charge-distribution among the layers of graphene due to the substrate effect on the bottom layer and adsorbed ammonia molecules on the top layer. Simultaneous measurements of Fano line shape and infrared signature of adsorbed ammonia molecules have also revealed the orientation of ammonia molecules on graphene and confirmed the charge-transfer mechanism of chemical doping.

DOI: 10.1103/PhysRevB.82.155435 PACS number(s): 73.22.Pr, 78.30.−j, 78.67.Wj

Graphene has attracted considerable interest for basic and applied research. Not only has graphene provided us with a unique arena to exploit theoretically and experimentally a variety of exotic properties of relativistic massless Fermion but it also enables numerous promising applications.[1] Optical technique, especially Fourier transform infrared spectroscopy (FTIR) has recently been employed to reveal the strong electron-phonon interaction in double-layer graphene through the observation of gate-controlled Fano resonance.[2–4] However, the reported phenomena required a high gate voltage and low temperature. These conditions limit further fundamental research and device applications of graphene, especially chemically synthesized graphene, which holds the promise for large-scale device applications.[5–9] In this work, we report the observation of room-temperature Fano resonance in few-layer graphene synthesized by chemical-vapor deposition (CVD). The infrared-active phonon and its associated Fano resonance are obtained using attenuated total reflectance (ATR) FTIR technique, which has been widely used to characterize chemically synthesized graphene before, but a clear phonon spectrum has not been observed.[8,10,11] The Fano resonance is confirmed by comparing the observed phonon line shape with calculation result. We show that the Fano line shape can be continuously tuned by ammonia chemical doping and the analysis of this line shape reveals different electron-phonon interaction in few-layer graphene than in double layer graphene.[3,4] By simultaneously monitoring the doping of graphene and the absorption spectrum of the adsorbed ammonia molecules, we have obtained the configuration of ammonia molecules on graphene and confirmed the charge-transfer mechanism of chemical doping.[12,13] Our observations demonstrate the potential of FTIR and Fano resonance in the fundamental study of electron-phonon interaction in graphene, and pave the way for the optoelectronic and sensing applications of graphene.

Graphene is synthesized on copper substrate by chemical-vapor deposition in a quartz tube furnace at ambient pressure,[14] a higher concentration of methane is used to obtain few-layer graphene. Raman scattering is used to characterize graphene, and it is performed at room temperature using a home-built system that consists of an optical microscope, a grating spectrometer (Triax 550, Horiba), and a liquid nitrogen-cooled charge-coupled device. A 532 nm solid-state laser is used as an optical excitation. Typical Raman spectra of the samples are shown in Fig. 1, characteristic of three-layer graphene.[6,15] Manual scanning of Raman spectra across the graphene film shows that ~70% of the sample is made of three-layer graphene, although random spots of thicker graphene can be observed. Room temperature polarity and carrier concentration of graphene as a function of NH_3 doping are obtained using the Van der Pauw structure Hall Effect. Fermi level is determined by measured carrier concentration, room-temperature Fermi-Dirac distribution, and the band structure of trilayer and four-layer graphene with Bernard stacking,[16] assuming 70% coverage of three-layer graphene and 30% coverage of four-layer graphene. FTIR measurement is taken with a Nicolet Magna equipped with a liquid-nitrogen-cooled HgCdTe detector.

Figure 2(a) shows FTIR spectra of few-layer graphene near the infrared active in-plane vibrational mode of graphite [Fig. 2(f)]. The asymmetric line shape is similar to Fano resonance observed in gated double-layer graphene[3,4] and this line shape is quite different from the absorption band of

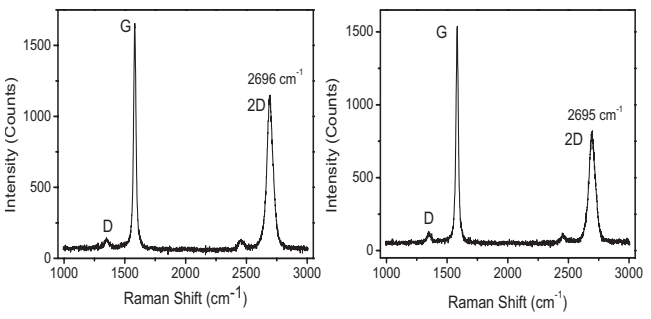

FIG. 1. Representative Raman spectra from three-layer regions of the few-layer graphene on ZnSe M-ATR crystal. The relative weak D line indicates the high quality of the transferred graphene.

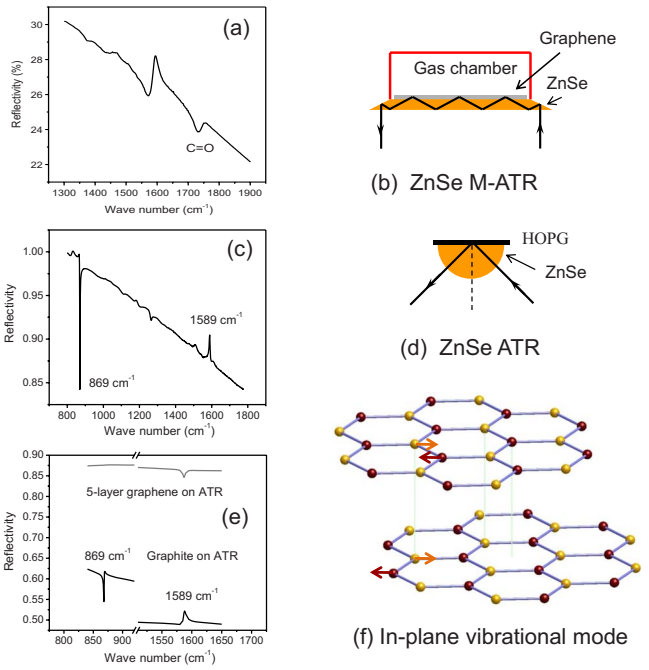

FIG. 2. (Color online) (a) Infrared spectrum of in-plane E_{1u} vibrational mode measured with M-ATR. Graphene was transferred to both the top and bottom surfaces of the ZnSe crystal of an M-ATR in order to increase the absorption signal, and measurement was performed in purging nitrogen. (b) Schematic of ZnSe M-ATR configuration. Graphene is transferred only to the top surface of ZnSe for the controlled NH_3 chemical doping. The NH_3 chamber has controlled flow input and output, and it can be detached from the M-ATR. (c) FTIR spectrum of HOPG with ZnSe single-bounce ATR. The near 100% reflectivity at 800 cm^{-1} is due to the drift and weak response of the detector. (d) Schematic of ZnSe single-bounce ATR for HOPG. (e) ZnSe single-bounce ATR phonon spectra of HOPG and five-layer graphene calculated using optical constants of HOPG. (f) Infrared-active in-plane lattice vibrational mode of double-layer and thicker graphene (Ref. 17).

C═O vibrational mode at ~1730 cm^{-1}.[11] The measurement was performed using a multibounce attenuated total reflectance (M-ATR) crystal at room temperature [Fig. 2(b)], where graphene is transferred to the top or both surfaces of the ZnSe crystal in order to increase the interaction length between light and graphene. The C═O signal comes mainly from chemical residues of polymethyl methacrylate, which is used in transferring graphene from the copper substrate to ZnSe ATR.[6,14]

In order to understand the origin of this abnormal phonon line shape and to eliminate the optical effect due to ATR configuration,[18] we first investigate the phonon spectra of graphite under similar configurations, and then calculate the phonon spectrum of few-layer graphene assuming no electron-phonon interaction. Figure 2(c) shows measured phonon spectra of highly ordered pyrolytic graphite (HOPG) using a single-bounce ZnSe ATR configuration as shown in Fig. 2(d).[19] Figure 1(e) shows the corresponding ATR spectra of HOPG and representative few-layer (five-layer) graphene calculated based on the matrix-transfer method and the optical constants of HOPG.[18,20] As can be seen, the calculated spectrum of HOPG captures very well the relative ratio and polarity of out-of-plane and in-plane phonon modes.[19] The difference in the background reflectivity between measurement and calculation is probably due to the following two factors: (1) the HOPG might have different optical constant as used in the calculation and (2) the HOPG may not have an intimate contact with ZnSe crystal in the measurement as assumed in the calculation.

The dependence of the polarity and ratio between the above two phonon modes is a typical example of optical effect due to reflectance configuration.[18] In a simple transmission configuration, infrared-active phonon will appear as a dip in the FTIR spectrum due to its optical absorption. This optical effect is further manifested as we calculate the phonon spectrum of few-layer (<100) graphene. First, the in-plane E_{1u} phonon at 1589 cm^{-1} of few-layer graphene shows a dip instead of a peak, as for HOPG. Second, the out-of-plane A_{1u} mode at 869 cm^{-1} does not exhibit a well-defined peak. Our calculation shows that the line shape of in-plane phonon begins to transform from a dip to a peak at about 100 layers while it is not until more than 180 layers that the out-of-plane phonon spectrum begins to appear as a negative peak. This thickness-dependent phonon line shape can be understood in the following way. For bulk HOPG with the ZnSe ATR technique, there is no internal reflection at the interface between ZnSe and graphite because of the smaller index of ZnSe, and such an obtained spectrum is similar to reflection spectroscopy.[19] However, for few-layer graphene, the total internal reflection happens at the interface between graphene and air, and light passes through graphene twice for each reflection, so the collected light can be treated as a transmitted beam, in other words, the ATR reflectivity spectrum of a very thin film should be identical to its transmission spectrum.[21] This conclusion is supported by the line shape of C═O absorption band in Fig. 1(a).

Based on the above results and discussions, we can conclude that the ATR-FTIR phonon spectrum without electron-phonon interaction should have a well-defined absorption band similar to that of the C═O bond, the observed abnormal line shape must be a manifestation of Fano resonance of E_{1u} phonon due to the strong electron-phonon interaction in graphene. On the other hand, we do not observe a clear absorption line shape for the out-of-plane vibrational mode. This result agrees with the calculation, implying that A_{1u} phonon does not have a strong interaction with electron. Fano resonance has been shown to be tuned by gate voltage.[3,4] Here, we demonstrate the tuning of Fano resonance by chemical doping. Figure 3 shows the change in phonon intensity and Fano line shape when NH_3 is used to progressively turn graphene from p type to n type.[12] The broadband background has been removed as a third-order polynomial determined outside the phonon peak.[3,4] The spectrum evolves from antiresonance to strong interference to phonon dominated as graphene is converted from heavily hole doped to heavily electron doped. The observed Fano line shape can be described by the following equation:[3,22]

$$T(\omega) = T_e\left[1 - \frac{(qr + \omega - \Omega)^2}{(\omega - \Omega)^2 + r^2}\right], \quad (1)$$

where Ω is the frequency of coupled or charged phonon, r is the phonon line width, and q is a dimensionless parameter

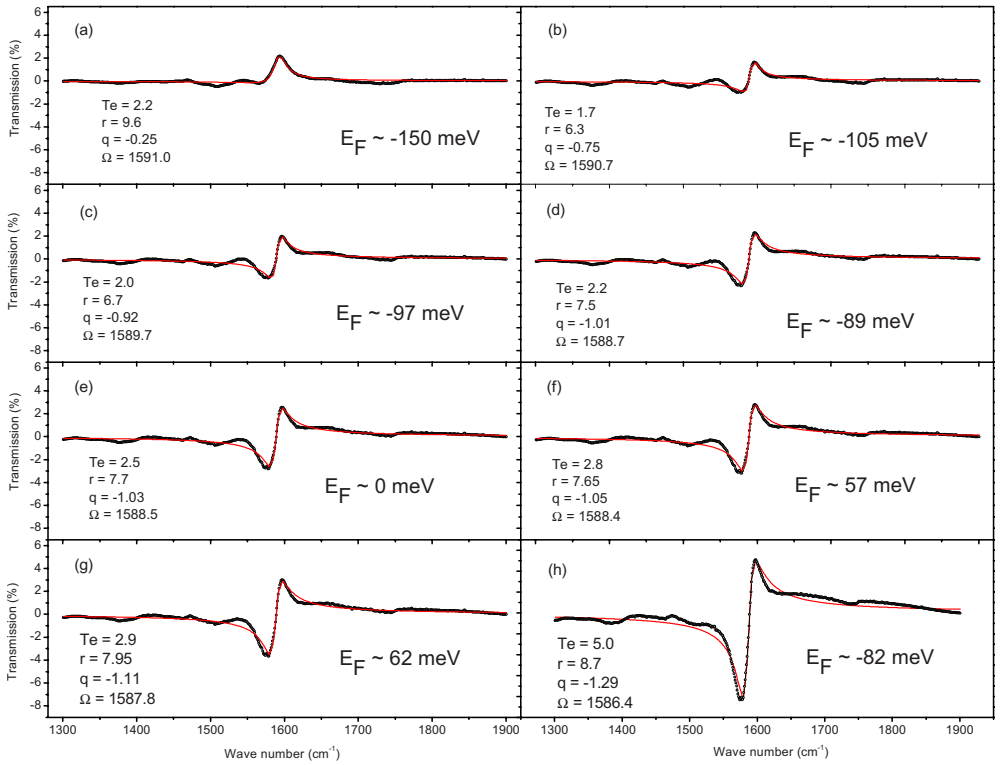

FIG. 3. (Color online) Evolution of phonon line shape and intensity as graphene is progressively transformed from *p* type to *n* type by NH_3 chemical doping. The doping level is controlled by NH_3 flow rate and flow duration. The red curves are fits with Fano parameters and approximate Fermi levels shown in each graph.

that depends on the coupling between phonon oscillation and continuum transitions as well as their relative strengths. As discussed before,[3] q is a negative number, and a Lorentzian absorption line shape is recovered as $|q| \gg 1$. T_e is called the bare electronic state absorption by Berkeley group,[3] but since the electronic background has been removed in the Eq. (1), T_e is related to the oscillator strength of the charged phonon because, equals to $\frac{\omega_p^2}{2\gamma \cdot q^2}$, where ω_p^2 is the plasma frequency of charged phonon defined by Geneva group.[4,23]

The dependencies of Fano parameters on Fermi level are summarized in Figs. 4(a)–4(d). It can be seen that all of these parameters behave quite differently from those reported in previous double-layer graphene.[3,4,23] Ω and q experience monotonic change as Fermi level rises from below to above the neutrality point: the magnitude of q increases from much less than 1 to greater than 1; the frequency of coupled phonon decreases from about 2 cm^{-1} above the phonon frequency of graphite to ~3 cm^{-1} below. Figure 3(d) shows that the line width of coupled phonon is greater than that of HOPG (~3 cm^{-1}), but it fluctuates between 6 and 10 cm^{-1}, and there is no significant increase near the neutrality point. In contrast, both groups have shown a much-enhanced linewidth when phonon is in resonance with continuum transition.[3,4] Finally, we observed that T_e is much larger in *n*-doped than *p*-doped graphene.

The behavior of Fano resonance and phonon intensity probably stem from band structure and electron-phonon interaction in three-layer graphene. As shown in Figs. 5(c)–5(e), there are different continuum transitions that have overlap in energy with phonon when the Fermi level is below, close to, or above the neutrality point, so there is always a strong coupling between phonon and electron-hole excitations. On the other hand, there is a clear asymmetry between hole-doped graphene and electron-doped graphene, as is re-

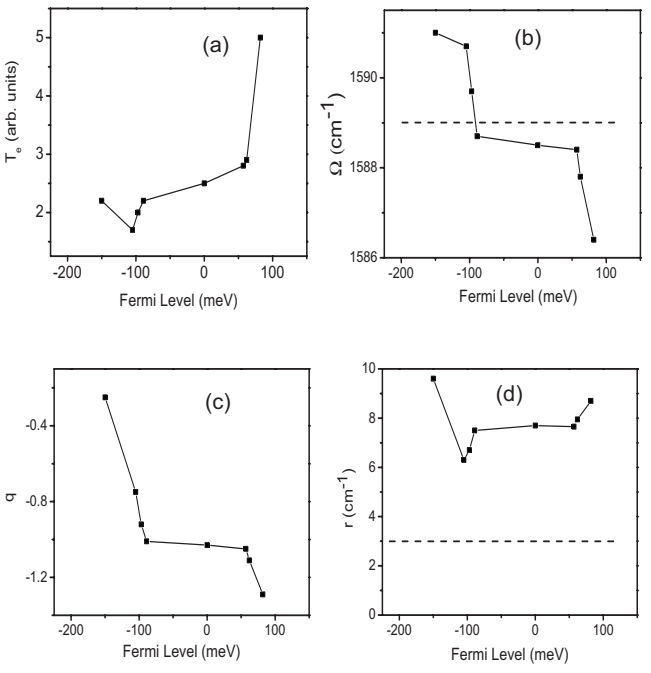

FIG. 4. Fano parameters as a function of Fermi level. Fano parameters are obtained from fits in Fig. 3. Dashed lines in (b) and (d) indicate the position and line width of phonon in HOPG, which are obtained from data in Fig. 2(c).

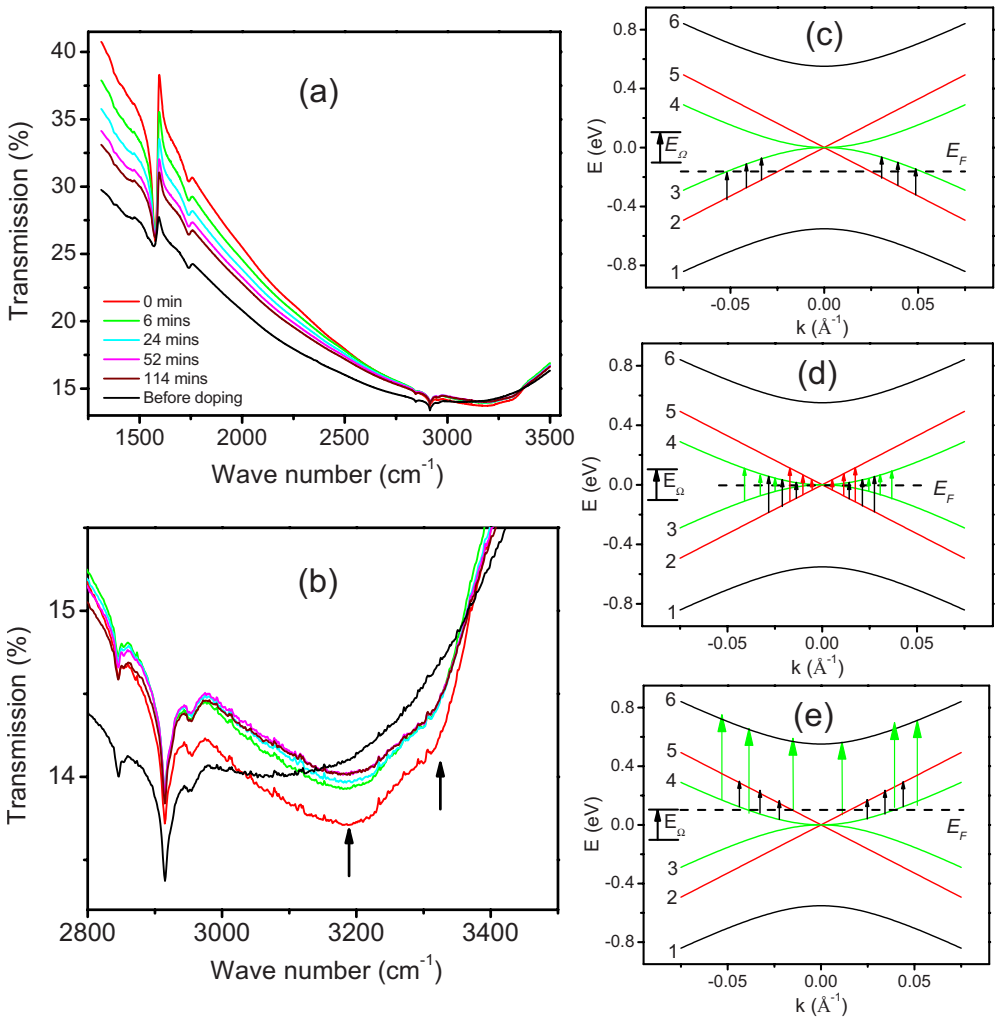

FIG. 5. (Color online) (a) FTIR spectral evolution of Fano resonance and NH_3 molecules adsorbed on graphene. Graphene is attached to both ZnSe M-ATR surfaces and is initially exposed to pure NH_3. FTIR measurement starts after M-ATR is taken out of the NH_3 chamber and NH_3 is allowed to leave the graphene surface into the air. (b) Closeup of the absorption band of adsorbed NH_3 near 3200 cm^{-1}. [(c)–(e)] Continuum of electronic transitions that could be resonantly coupled to phonon excitation when Fermi levels are at (c) $E_F \sim -E_\Omega/2$, (d) $E_F \sim 0$, and (e) $E_F \sim E_\Omega/2$.

flected on the behavior of Ω and T_e. The continuous redshift of Ω and enhanced strength of T_e in increased electron doping indicate that phonon is coupled to the transitions between bands 4, 5, and band 6 [Fig. 5(e)].[4,24] Similar phonon behaviors have been observed in electron-doped alkali-C_{60} compounds and is attributed to the charged-phonon effect.[4,25,26] A number of chemicals other than NH_3 and NO_2 have recently been reported to make graphene *n* type or *p* type.[27] Br_2 and I_2 have been shown to *p*-doped graphene to a level that cannot be achieved by the electrode gating.[28] It is anticipated that more pronounced phonon intensity will be observed in more heavily doped graphene.

The asymmetric dependence of Fano resonance on the type of doping could also arise from asymmetric distribution of charge among different layers of graphene. Substrate is believed to partly attribute to the *p* doping of graphene.[29] *N*-type chemical doping could result in a high density of electron on the layer of graphene that adsorbs ammonia molecules.[28] Further investigation is required to obtain a better picture of charge distribution in few-layer-doped graphene.

The doping-sensitive Fano resonance also helps to shed light on the doping mechanism of NH_3.[12,30] Theoretical calculation shows that *n* doping is due to the charge transfer from adsorbed NH_3 to graphene and that NH_3 molecules are oriented on the graphene surface in such a way that H atoms are pointed away from the graphene surface.[13] This picture is supported by our observation. Figures 5(a) and 5(b) shows a series of Fano resonance spectra as NH_3 molecules diffuse away from the graphene surface. We can observe a direct correlation between electron density and the absorption bands centered at 3220 and 3310 cm^{-1}. These broad absorption bands are due to the N—H stretching modes of $-NH_3$.[31–33]

In conclusion, we have observed optical phonon spectrum and Fano-type phonon resonance in few-layer CVD graphene using room-temperature infrared spectroscopy. We have also shown that the Fano line shape and phonon oscil-

lator strength can be controlled by chemical doping but with different behaviors than previously reported in double-layer graphene.[3,4] The simultaneous FTIR measurement of doping-dependent phonon spectrum and adsorbed chemical species can be used to understand the sensing and doping mechanisms of other chemicals adsorbed on graphene. The observations of phonon spectrum and controlled Fano resonance at room temperature allow us to characterize lattice structure, doping level and to understand the complicated nature of electron phonon in graphene. Our findings and FTIR technique have paved the way for device applications of large-area chemically synthesized graphene.

ACKNOWLEDGMENTS

Financial supports from the National Science Foundation under Grant No. NSF/DMR-0907336, Texas Center for Superconductivity at Houston (TcSUH), and from the Robert A. Welch Foundation (E-1728) are greatly acknowledged. The authors thank Benfatto for sharing their latest theoretical work and for pointing out the correct definition of phonon oscillator strength (Ref. 23).

*qingkai.yu@mail.uh.edu
†jbao@uh.edu

[1] A. H. Castro Neto, F. Guinea, N. M. R. Peres, K. S. Novoselov, and A. K. Geim, Rev. Mod. Phys. **81**, 109 (2009).
[2] S. Pisana, M. Lazzeri, C. Casiraghi, K. S. Novoselov, A. K. Geim, A. C. Ferrari, and F. Mauri, Nature Mater. **6**, 198 (2007).
[3] T. Tang, Y. Zhang, C.-H. Park, B. Geng, C. Girit, Z. Hao, M. C. Martin, A. Zettl, M. F. Crommie, S. G. Louie, Y. R. Shen, and F. Wang, Nat. Nanotechnol. **5**, 32 (2010).
[4] A. B. Kuzmenko, L. Benfatto, E. Cappelluti, I. Crassee, D. van der Marel, P. Blake, K. S. Novoselov, and A. K. Geim, Phys. Rev. Lett. **103**, 116804 (2009).
[5] Q. K. Yu, Y. Zhang, C.-H. Park, B. Geng, C. Girit, Z. Hao, M. C. Martin, A. Zettl, M. F. Crommie, S. G. Louie, Y. R. Shen, and F. Wang, Appl. Phys. Lett. **93**, 113103 (2008).
[6] X. S. Li, W. Cai, J. An, S. Kim, J. Nah, D. Yang, R. Piner, A. Velamakanni, I. Jung, E. Tutuc, S. K. Banerjee, L. Colombo, and R. S. Ruoff, Science **324**, 1312 (2009).
[7] A. Reina, X. Jia, J. Ho, D. Nezich, H. Son, V. Bulovic, M. S. Dresselhaus, and J. Kong, Nano Lett. **9**, 30 (2009).
[8] Y. Hernandez, V. Nicolosi, M. Lotya, F. M. Blighe, Z. Sun, S. De, I. T. McGovern, B. Holland, M. Byrne, Y. K. Gun'Ko, J. J. Boland, P. Niraj, G. Duesberg, S. Krishnamurthy, R. Goodhue, J. Hutchison, V. Scardaci, A. C. Ferrari, and J. N. Coleman, Nat. Nanotechnol. **3**, 563 (2008).
[9] K. V. Emtsev, A. Bostwick, K. Horn, J. Jobst, G. L. Kellogg, L. Ley, J. L. McChesney, T. Ohta, S. A. Reshanov, J. Röhrl, E. Rotenberg, A. K. Schmid, D. Waldmann, H. B. Weber, and T. Seyller, Nature Mater. **8**, 203 (2009).
[10] D. Li, M. B. Müller, S. Gilje, R. B. Kaner, and G. G. Wallace, Nat. Nanotechnol. **3**, 101 (2008).
[11] Y. Si and E. T. Samulski, Nano Lett. **8**, 1679 (2008).
[12] F. Schedin, M. B. Müller, S. Gilje, R. B. Kaner, and G. G. Wallace, Nature Mater. **6**, 652 (2007).
[13] O. Leenaerts, B. Partoens, and F. M. Peeters, Phys. Rev. B **77**, 125416 (2008).
[14] H. L. Cao, Q. Yu, L. A. Jauregui, J. Tian, W. Wu, Z. Liu, R. Jalilian, D. K. Benjamin, Z. Jiang, J. Bao, S. S. Pei, and Y. P. Chen, Appl. Phys. Lett. **96**, 122106 (2010).
[15] A. C. Ferrari, J. C. Meyer, V. Scardaci, C. Casiraghi, M. Lazzeri, F. Mauri, S. Piscanec, D. Jiang, K. S. Novoselov, S. Roth, and A. K. Geim, Phys. Rev. Lett. **97**, 187401 (2006).
[16] F. Guinea, A. H. Castro Neto, and N. M. R. Peres, Phys. Rev. B **73**, 245426 (2006).
[17] Y. Wang, D. C. Alsmeyer, and R. L. McCreery, Chem. Mater. **2**, 557 (1990).
[18] K. Yamamoto and H. Ishida, Vib. Spectrosc. **8**, 1 (1994).
[19] T. Leitner, J. Kattner, and H. Hoffmann, Appl. Spectrosc. **57**, 1502 (2003).
[20] E. Palik, *Handbook of Optical Constants of Solids II* (Academic Press, New York, 1991).
[21] N. J. Harrick, J. Phys. Chem. **64**, 1110 (1960).
[22] U. Fano, Phys. Rev. **124**, 1866 (1961).
[23] E. Cappelluti, L. Benfatto, and A. B. Kuzmenko, Phys. Rev. B **82**, 041402(R) (2010).
[24] T. Ando, J. Phys. Soc. Jpn. **76**, 104711 (2007).
[25] K. J. Fu, W. L. Karney, O. L. Chapman, S. M. Huang, R. B. Kaner, F. Diederich, K. Holczer, and R. L. Whetten, Phys. Rev. B **46**, 1937 (1992).
[26] M. J. Rice and H. Y. Choi, Phys. Rev. B **45**, 10173 (1992).
[27] D. B. Farmer, R. Golizadeh-Mojarad, V. Perebeinos, Y.-M. Lin, G. S. Tulevski, J. C. Tsang, and P. Avouris, Nano Lett. **9**, 388 (2009).
[28] N. Jung, N. Kim, S. Jockusch, N. J. Turro, P. Kim, and L. Brusm, Nano Lett. **9**, 4133 (2009).
[29] S. Berciaud, S. Ryu, L. E. Brus, and T. F. Heinz, Nano Lett. **9**, 346 (2009).
[30] T. Lohmann, K. von Klitzing, and J. H. Smet, Nano Lett. **9**, 1973 (2009).
[31] J. Zawadzki and A. Wisniewski, Carbon **41**, 2257 (2003).
[32] M. D. Ellison, M. J. Crotty, D. Koh, R. L. Spray, and K. E. Tate, J. Phys. Chem. B **108**, 7938 (2004).
[33] A. Lubezky, L. Chechelnitsky, and M. Folman, Surf. Sci. **454-456**, 147 (2000).